Immunolocalization of the Ca2+-Activated K+ Channel Slo1 in Axons and Nerve Terminals of Mammalian Brain and Cultured Neurons

Hiroaki Misonou[1,2], **Milena Menegola**[1], **Lynn Buchwalder**[2], **Eunice W. Park**[2], **Andrea Meredith**[3], **Kenneth J. Rhodes**[4], **Richard W. Aldrich**[3], and **James S. Trimmer**[1,2]

[1]Department of Pharmacology, School of Medicine, University of California, Davis, CA 95616

[2]Department of Biochemistry and Cell Biology, State University of New York at Stony Brook, Stony Brook, NY 11794

Department of Molecular and Cellular Physiology and Howard Hughes Medical Institute, Stanford School of Medicine, Stanford, CA 94305

[4]Neuroscience, Wyeth Discovery Research, Princeton, New Jersey 08543

Abstract

Ca^{2+}-activated voltage-dependent K$^+$ channels (Slo1, KCa1.1, Maxi-K, or BK channel) play a crucial role in controlling neuronal signaling by coupling channel activity to both membrane depolarization and intracellular Ca^{2+} signaling. In mammalian brain, immunolabeling experiments have shown staining for Slo1 channels predominantly localized to axons and presynaptic terminals of neurons. We have developed anti-Slo1 mouse monoclonal antibodies that have been extensively characterized for specificity of staining against recombinant Slo1 in heterologous cells, and native Slo1 in mammalian brain, and definitively by the lack of detectable immunoreactivity against brain samples from Slo1 knockout mice. Here we provide precise immunolocalization of Slo1 in rat brain with one of these monoclonal antibodies and show that Slo1 is accumulated in axons and synaptic terminal zones associated with glutamatergic synapses in hippocampus and GABAergic synapses in cerebellum. By using cultured hippocampal pyramidal neurons as a model system, we show that heterologously expressed Slo1 is initially targeted to the axonal surface membrane, and with further development in culture, become localized in presynaptic terminals. These studies provide new insights into the polarized localization of Slo1 channels in mammalian central neurons and provide further evidence for a key role in regulating neurotransmitter release in glutamatergic and GABAergic terminals.

Keywords

BK channel; ion channel; localization; protein trafficking; mAb

INTRODUCTION

The somata, dendrites, and axons of mammalian central neurons express a wide array of voltage-gated ion channels. The distributions or densities of many of these channels in the neuronal membrane can be quite non-uniform (Trimmer and Rhodes, 2004). Large-

Correspondence to: James S. Trimmer, Department of Pharmacology, School of Medicine, GBSF 3503, University of California, One Shields Ave., Davis, CA, 95616. E-mail: jtrimmer@ucdavis.edu.
Associate editor: Oswald Steward, Ph.D.

conductance voltage-and Ca^{2+}-activated Slo1 K^+ channels (also known as KCa1.1, BK or Maxi-K channels) are ion channels that play especially critical roles in neuronal function based on their role as coincidence detectors whose function is controlled by both membrane potential and $[Ca^{2+}]_i$. Slo1 channels have been detected electrophysiologically as playing important roles in mammalian central neuron somata, dendrites and presynaptic terminals (e.g. Hu et al., 2001; Edgerton and Reinhart, 2003). Slo1 channels are composed of tetramers of pore-forming, and voltage- and Ca^{2+}-sensing, Slo1 (KCa1.1) α subunits (the product of the KCNMA1 gene), with or without auxiliary transmembrane β subunits (Orio et al., 2002). Slo1-containing channels contribute to diverse aspects of neuronal function, including neurotransmitter release, afterhyperpolarizations, and repolarization (Sah and Faber, 2002). Alternative splicing of KCNMA1 transcripts can generate a large number of distinct Slo1 polypeptides, including 16 known Slo1 isoforms in rat and mouse (NCBI Entrez Protein Database October 2005), many of which exhibit distinct functional characteristics (Shipston, 2001; Fury et al., 2002; Chen et al., 2005). Activity of Slo1-containing channels can be further modulated by dynamic changes in phosphorylation state (Weiger et al., 2002), and splicing at particular sites can influence the extent and nature of such modulation (Tian et al., 2001; Zhou et al., 2001). Consequently, Slo1-containing channels represent fundamental yet highly variable and dynamic regulators of membrane excitability.

There are several reports of Slo1 localization in brain using rabbit polyclonal antibodies (Table I) raised against synthetic peptides (Knaus et al., 1996;Hu et al., 2001;Grunnet and Kaufmann, 2004;Martin et al., 2004) or fusion proteins (Sausbier et al., 2004) corresponding to segments from the Slo1 α subunit intracellular C-terminus. The results obtained in these studies are consistent in showing Slo1 staining in brain regions rich in axons and presynaptic terminals, a localization that has also been verified at the electron microscope level, at least in hippocampal CA3 pyramidal cell Schaffer collateral presynaptic terminals (Hu et al., 2001). However, in some reports (e.g. Grunnet and Kaufmann, 2004;Martin et al., 2004) the Slo1 α subunit has also been described as having an extensive somatodendritic localization. To confirm and extend these studies, we have generated anti-Slo1 mouse monoclonal antibodies (mAbs), since (1) they provide continuous and consistent supply of mAbs and thus consistent results, (2) they can have greater specificity over polyclonal antibodies, and (3) the concentration of antibodies can be easily controlled to achieve the highest sensitivity and the lowest background. Here we provide detailed analyses of Slo1 localization in rat and mouse brain by using a specific mAb generated against Slo1, whose specificity has been validated by a number of assays including a lack of detectable immunoreactivity against samples from Slo1 knockout mice. We also characterize the localization of exogenously expressed Slo1 α subunits in hippocampal neurons developing in culture that exhibit a prominent localization of Slo1 in axons and presynaptic terminals.

MATERIALS AND METHODS

Monoclonal antibody production

L6/60 mAbs against the Slo1 channel α subunit were raised against a GST-mSlo1 fusion protein corresponding to amino acids 690–1196 of mSlo1. Note that positions given here differ from those reported in Pyott et al., (2004) to unambiguously correspond to amino acid positions of the original mSlo cDNA MBR5, accession number AAA39746 (Butler et al., 1993), now referred to as mouse KCMA1 isoform 2 in the KCMA1 protein reference sequence accession Q08460. The amino acid numbering of reference sequence AAA39746 will be used throughout this report. Hybridomas secreting L6/60 mAbs were generated as described previously (Bekele-Arcuri et al., 1996). Hybridoma clones were screened by chemiluminescence enzyme-linked immunosorbant assay (ELISA) against COS-1 cells expressing full length human Slo1 (Meera et al., 1997), and then further selected based on

immunofluorescence staining of COS-1 cells transfected with the same human Slo1 cDNA. The original ELISA assay yielded 77 positives, of which 53 replicated in the COS immunofluorescence staining. Further screening of these 53 positive clones revealed 14 that yielded single Slo1-sized bands on immunoblot analyses of adult rat brain membrane fractions, and 19 that yielded acceptable immunoperoxidase staining of rat brain sections. Of these, L6/60 (of mouse IgG$_{2a}$ subtype) was chosen for the studies below. The binding site of L6/60 was further defined by ELISA and immunoblots as being located within amino acids 690–891 of mSlo1 (accession number AAA39746; Butler et al., 1993).

Other antibodies used in this study

Trimmer lab antibodies

K14/16: described in detail in Bekele-Arcuri et al. (1996). Mouse monoclonal IgG2b antibody generated against a recombinant GST fusion protein (GST-RAK) containing amino acids 428–499 of rat Kv1.2. Binding site subsequently mapped to within amino acids 463–480. No crossreactivity against other Kv1 family members (Kv1.1, Kv1.3, Kv1.4, Kv1.5 and Kv1.6 overexpressed in heterologous cells (Bekele-Arcuri et al., 1996). Immunoblots yield a major population of Kv1.2 with processed N-oligosaccharides, and a minor population with high mannose oligosaccharides (Bekele-Arcuri et al., 1996; Shi et al., 1999). Immunoblot staining eliminated by preincubation with GST-RAK (Bekele-Arcuri et al., 1996). Staining pattern in brain sections (Bekele-Arcuri et al., 1996; Rhodes et al., 1997; Monaghan et al., 2000) consistent with published (Tsaur et al., 1992; Veh et al., 1995) and unpublished (K. J. Rhodes) *in situ* hybridization data, and with published light and electron microscopic level reports of Kv1.2 localization (McNamara et al., 1993; Wang et al., 1993, 1994).

K13/31: described in detail in Bekele-Arcuri et al. (1996). Mouse monoclonal IgG1 antibody generated against a synthetic peptide (Kv1.4N) corresponding to amino acids 13–37 of rat Kv1.4, identical to that used previously to generate a specific anti-Kv1.4 rabbit polyclonal antibody (Sheng et al., 1992). No crossreactivity against other Kv1 family members (Kv1.1, Kv1.2, Kv1.3, Kv1.5 and Kv1.6 overexpressed in heterologous cells (Bekele-Arcuri et al., 1996). Immunoblots yield a major population of Kv1.4 with processed N-oligosaccharides, and a minor population with high mannose oligosaccharides (Bekele-Arcuri et al., 1996; Shi et al., 1999). Immunoblot staining eliminated by preincubation with Kv1.4N peptide (Bekele-Arcuri et al., 1996). Staining pattern in brain sections (Bekele-Arcuri et al., 1996; Rhodes et al., 1997; Monaghan et al., 2000) consistent with published (Veh et al., 1995) and unpublished (K. J. Rhodes) *in situ* hybridization data, and with published light and electron microscopic level reports of Kv1.4 localization (Sheng et al., 1992; Maletic-Savatic et al., 1995; Cooper et al., 1998).

K28/43: described in detail in Tiffany et al. (2000) and Rasband et al. (2002). Mouse monoclonal IgG2a antibody generated against a recombinant GST fusion protein (GST-KAP1.13) containing amino acids 77–299 of human PSD-95, identical to that used previously to generate a specific anti-PSD-95 guinea pig polyclonal antibody (Kim et al., 1995). No crossreactivity against other membrane-associated guanylate kinases (SAP97, Chapsyn-110, SAP102 overexpressed in heterologous cells (Rasband et al., 2002). Immunoblot staining eliminated in a transgenic mouse expressing a truncated version of PSD-95 (Rasband et al., 2002). Staining pattern in brain sections (Rasband et al., 2002) consistent with published light and electron microscopic level reports of PSD-95 localization (Sheng et al., 1995; Peterson et al., 2003).

K89/41: Mouse monoclonal IgG1 antibody generated against a synthetic peptide (KC) corresponding to amino acids 837–853 of rat Kv2.1, identical to that used to generate Kv2.1-specific polyclonal antibodies (Trimmer, 1991; Hwang et al., 1993). Immunoblots yield a

single Kv2.1 band (Misonou et al., 2004). Staining pattern in brain sections (Misonou et al., 2004) consistent with published (Drewe et al., 1992) and unpublished (K. J. Rhodes) *in situ* hybridization data, and with published light and electron microscopic level reports of Kv2.1 localization ((Trimmer, 1991; Hwang et al., 1993; Maletic-Savatic et al., 1995; Rhodes et al., 1997; Du et al., 1998; Monaghan et al., 2000).

L11A/41: described in detail in Schafer et al (2004). Mouse monoclonal IgG1 antibody generated against a recombinant GST fusion protein containing amino acids 1066–1174 of rat neurofascin-155 (NF-155), and common to NF-186. Recognizes both major splice variants of neurofascin (NF-155, NF186) on immunoblots. Preincubation of L11A/41 with the immunizing fusion protein abolished all immunoreactivity (Schafer et al., 2004). Staining pattern in brain sections consistent with that of a combination of NF-155 (Collinson et al., 1998) and NF-186 (Davis et al., 1996)

KC: described in detail in Trimmer, 1991. Rabbit polyclonal affinity-purified antibody generated and affinity purified against a synthetic peptide (KC) corresponding to amino acids 837–853 of rat Kv2.1, identical to that used to generate another Kv2.1-specific polyclonal antibody (Hwang et al., 1993). No crossreactivity against Kv2.2 (Lim et al., 2000)). Immunoblots yield a single Kv2.1 band (Trimmer, 1991; Shi et al., 1999). Immunoblot staining eliminated by preincubation with KC peptide (Trimmer, 1991). Staining pattern in brain sections (Trimmer, 1991; Maletic-Savatic et al., 1995; Rhodes et al., 1997; Monaghan et al., 2000) consistent with published (Drewe et al., 1992) and unpublished (K. J. Rhodes) *in situ* hybridization data, and with published light and electron microscopic level reports of Kv2.1 localization (Hwang et al., 1993; Du et al., 1998).

Antibodies obtained from other sources

Calbindin D-28K: Sigma C9848. Mouse monoclonal IgG1 antibody generated against purified bovine kidney calbindin-D. Does not react with other members of the EF-hand family, such as calbindin-D-9K, calretinin, myosin light chain, parvalbumin, S-100a, S-100b, S-100A2 (S100L) and S-100A6 (calcyclin).

GluR1: Upstate Biotech 07-660. Rabbit protein A purified polyclonal antibody generated against a synthetic peptide corresponding to amino acids 276–287 of rat glutamate receptor 1 (GluR1). Yields a single 106 kD band on immunoblots of rat brain microsomal membranes.

MAP2: Sigma M1406. Mouse monoclonal IgG1 antibody generated against purified bovine MAP2 (Binder et al., 1986). Recognizes an epitope on the high molecular weight MAP2 forms, MAP2a and MAP2b and shows no reaction with the low molecular weight MAP2c or other microtubule proteins.

Myc 1-9E10: ATCC CRL-1729. Mouse monoclonal IgG1 antibody generated against a synthetic peptide (peptide G) corresponding to amino acids 408–432 of human p62 c-myc (Evan et al., 1985). The antibody precipitates the human c-myc protein, but does not react with mouse or chicken c-myc.

Synapsin I: Sigma S193. Rabbit polyclonal affinity-purified antibody generated against purified bovine brain synapsin I. Strongly reacts with synapsin Ia and Ib (De Camilli et al., 1983).

Tau: Chemicon Mab3420, clone Tau-1, PC1C6. Mouse monoclonal IgG2a antibody generated against purified denatured bovine brain microtubule associated proteins (Binder et

al., 1985). Recognizes all known electrophoretic species of tau in human, rat and bovine brain (Szendrei et al., 1993).

Neuronal culture

Dissociated cultures of embryonic rat hippocampal neurons were prepared as previously described (Banker and Cowan, 1977; Misonou et al., 2004; Misonou and Trimmer, 2005). Briefly, hippocampi from 18 or 19-day rat embryos were dissociated by treatment with trypsin (0.25% w/v) for 15 min at 37°C followed by triturating with a constricted Pasteur pipet. The cells were diluted in modified Eagle's medium (Invitrogen) containing 10% (v/v) horse serum, 0.06% (v/v) glucose and plated on 22 mm square coverslips coated with 1 mg/ml poly-L-lysine. After 4 h, when the cells were adhered to the substrate, the coverslips were transferred into 6-well tissue culture plates which contained a confluent layer of astrocytes prepared from cerebral hemispheres of neonatal rat pups in serum-free modified Eagles medium with N2 supplements, 0.1% (w/v) ovalbumin and 0.1 mM sodium pyruvate (Banker and Cowan, 1977). After 3 days, 1 µM cytosine arabinoside was added to inhibit proliferation of non-neuronal cells. Cultures were kept at 37°C in a humidified atmosphere of 95% air and 5% CO_2. Neurons cultured for 8 days were transfected with human Slo1 cDNA with an extracellular Myc tag (Hf1) (Meera et al., 1997) using Lipofectamine2000 (Invitrogen) as described (Lim et al., 2000).

Immunostaining of rat brain sections

All animal use procedures were in strict accordance with the Guide for the Care and Use of Laboratory Animals described by the National Institutes of Health. Rats were anesthetized with 60 mg/Kg pentobarbital (i.p.) and briefly perfused with a saline solution followed by a 4% paraformaldehyde in phosphate buffer. Sagittal brain sections (40 µm thick) were prepared as described (Rhodes et al., 1997). Brain sections were permeabilized with 0.1% Triton X-100 in Tris-buffered saline (TBS, 10 mM Tris, pH 7.5/0.15 M NaCl). For the diaminobenzidine/nickel ammonium sulfate staining sections were blocked in a 5% horse serum solution, incubated overnight with L6/60 mAb (0.6 µg/ml), and 1 h in biotinylated horse anti-mouse secondary antibody (Vector Laboratories, Burlingame, CA). Detection of the antibody-antigen complexes was accomplished using the ABC Elite peroxidase reaction kit (Vector Laboratories, Burlingame CA) and visualized using nickel-enhanced diaminobenzidine procedure.

For the immunofluorescence staining, sections were blocked with 10% goat serum solution, then incubated overnight at 4°C with L6/60 mAb (24 µg/ml), and 1) mouse mAbs raised against either Kv1.2 (K14/16, Bekele-Arcuri et al., 1996, 16 µg/ml), Kv1.4 (K13/31, Bekele-Arcuri et al., 1996; TC supe 1:2), neurofascin NF-155/186 (L11A/41, Boiko et al., 2003, TC supe 1:2) or calbindin D-28K (CB-955; Sigma C9848, lot 113K4867, 16 µg/ml) or 2) rabbit KC polyclonal antibodies raised against Kv2.1 (Trimmer, 1991, 1:100). Sections were then incubated with species- or isotype-specific Alexa-conjugated secondary antibodies (Molecular Probes) as described elsewhere (Strassle et al., 2005). Fluorescent images were taken with a 24-bit color digital camera installed on a Carl Zeiss Axiovert 200M microscope with a 63x, 1.3 numerical aperture lens and Apotome, using Axiovision software.

Experimental localization of Slo1

Experimental lesions of the rat dentate gyrus were performed as described (Monaghan et al., 2001). All surgical procedures were approved by the Wyeth-Ayerst Institutional Animal Care and Use Committee and were in accordance with the National Institutes of Health Guide for the Care and Use of Laboratory Animals. Before surgery, animals were deeply anesthetized with sodium pentobarbital (50 mg/kg, i.p.) and secured in a stereotaxic carrier

(David Kopf Instruments, Tajunga, CA). For lesions of the dentate gyrus, ibotenic acid (0.1–0.4 µl of a 10 µg/µl solution in 0.1 M sodium phosphate buffer, pH 7.4) was injected directly into the target structure using a 2 µl Hamilton (Reno, NV) microsyringe mounted in a Kopf microsyringe microdrive. In some of these animals, injections were made at two or three depths, with each injection separated in the dorsoventral axis by 2.5 mm. Animals were used for immunostaining, as described above, except using L6/60 and K13/31 TC supe at 1:10 dilution, after a 7 d postsurgical survival period.

Immunofluorescence staining of cultured neurons

At 11 or 14 days *in vitro* (DIV), neurons were fixed with 4% paraformaldehyde in PBS containing 4% sucrose for 20 min at 4°C. Cells were blocked with 4% nonfat dry milk powder in TBS (Blotto-TBS) for 30 min and then incubated with mouse anti-c-Myc mAb (19E10; antibody purified from ascites fluid grown from hybridomas obtained from American Type Culture Collection, 1 µg/ml) for surface labeling of hSlo1. Cells were then incubated in Blotto-TBS containing 0.1% Triton X-100 for 30 min at room temperature and probed with mouse mAbs L6/60 (24 µg/ml), anti-Myc (1-9E10, ATCC, 1 µg/ml), anti-PSD95 (K28/43; Tiffany et al., 2000; Rasband et al., 2002, TC supe 1:10), anti-tau (Chemicon Mab3420, 1:2000) or anti-MAP-2 (Sigma M1406, 1:1000), or rabbit anti-synapsin I (Sigma S193, 1:1000). The specimens were incubated with Alexa-conjugated secondary antibodies and 10 µg/ml Hoechst 33258 (Molecular Probes). Images were taken with a 24-bit color digital camera installed on a Carl Zeiss Axioskop 2 microscope using Axiovision software (Carl Zeiss). Images were transferred to Adobe PhotoShop software (Adobe Systems, San Jose, CA) as JPEG files.

Immunoblots

Rat and brain membranes were prepared and treated with purified alkaline phosphatase (AP) as previously described (Shi et al., 1994; Murakoshi et al., 1997; Misonou et al., 2004). In brief, brains from different ages of rats were homogenized in 5 mM phosphate buffer (pH7.4) containing 320 mM sucrose, 100 mM NaF. The homogenate was centrifuged at 800 × g for 10 min to remove nuclei and unbroken tissues, and then centrifuged at 100,000 × g to prepare a membrane fraction. For alkaline phosphatase digestion, rat brain membrane fractions were washed twice with 5 mM phosphate buffer (pH7.4) by centrifugation and resuspension in the same buffer to give a final 10 mg/ml protein concentration. Membranes were then diluted with AP buffer (Roche), to yield a final reaction mixture at 1.5 mg/ml protein concentration, to which protease inhibitors, 0.1% SDS, and 0.1 U/ml AP were added and incubated for 3 h at 37 °C. Digested and undigested membranes were diluted with the sample buffer for SDS-PAGE. Mouse brain membranes were prepared from brains of Slo1-knockout mice and wild-type littermates (Meredith et al., 2004). Molecular weight standards were Amersham Rainbow Markers (RPN800) or Sigma Prestained Molecular Weight Markers (SDS-7B). Proteins were separated on 7.5% SDS polyacrylamide gels (SDS-PAGE) and transferred to nitrocellulose membrane, and immunoblotted with L6/60 (10 µg/ml), anti-Kv2.1 (K89/41 mouse mAb, Antonucci et al., 2001, TC supe, 1:2;), anti-Kv1.4 (K13/31 mouse mAb, Bekele-Arcuri et al., 1996; TC supe 1:2), anti-GluR1 (rabbit polyclonal antibody, Upstate Biotech 07-660, 1:1000), or commercial anti-Slo1 rabbit polyclonal antibodies from Chemicon (AB5228, lot 22040170; 1:2000) or Alomone Labs (APC-021, lot AN-04, 1:500). The blots were incubated with HRP-conjugated secondary antibodies (ICN) followed by enhanced chemiluminescence reagent (Perkin Elmer). Immunoreactive bands were visualized by exposing the blot to X-ray film.

RESULTS

Characterization of mouse anti-Slo1 monoclonal antibodies

We developed a panel of mouse mAbs specific for the mouse Slo1 (mSlo) α subunit, raised against a recombinant fragment (Pyott et al., 2004) corresponding to amino acids 690–1196 of mSlo (accession number AAA39746; Butler et al., 1993). This large mouse Slo1 fragment, derived from the intracellular C-terminus is highly conserved in the rat (100% amino acid identity) and human (99% amino acid identity) Slo1 α subunit polypeptides. The resulting mAbs were extensively characterized for their specificity by immunofluorescence staining against recombinant Slo1 expressed in transfected cell lines, and immunoblotting and immunohistochemical staining of brain samples from adult rats. Ultimate validation was provided by analyzing samples from adult wild-type and Slo1-knockout mice (Meredith et al., 2004). As shown in Fig. 1, in rat and mouse brain samples L6/60 detected a single microheterogeneous protein band with a relative molecular mass (M_r) of ≈135 kD, consistent with the range of Slo1 isoforms in rat (1180–1210 amino acids) and mouse (1144–1209 amino acids). This immunoblot signal is completely absent in the samples from Slo1-deficient mice (Fig. 1). In parallel immunoblots, we tested commercially available anti-Slo1 antibodies (Table I) against these same samples. Surprisingly, these commercial antibodies recognize prominent bands in addition to the Slo1-sized band recognized by the L6/60 mAb, and the intensity of immunoreactivity to these extraneous bands is not diminished in the samples prepared from the Slo1 knockout mice (Fig. 1), suggesting that they are not the products of the Slo1/KCMA1 gene. These results demonstrate the exquisite specificity of the L6/60 antibody against Slo1 α subunit molecules in biochemical analyses of brain samples.

To begin to investigate the molecular basis of the observed microheterogeneity in the brain Slo1 pool on SDS gels, we subjected the adult rat brain membranes to alkaline phosphatase (AP) digestion. Treatment with AP led to a marked shift in the M_r of the component Slo1 bands (Fig. 2A). However, unlike previous results for the Kv2.1 channel (Murakoshi et al., 1997;Misonou et al., 2004), for which AP treatment leads to a complete loss of microheterogeneity of the brain Kv2.1 pool (Fig. 2A), the brain Slo1 population exhibits multiple bands even after extensive AP treatment (3 h at 37°C). This suggests that mechanisms outside of differential phosphorylation (e.g. alternative splicing of Slo1 mRNAs; Shipston, 2001) contribute to the microheterogeneity of the Slo1 polypeptide pool in rat brain that is observed on SDS gels. The immunoreactivity of L6/60 to multiple Slo1 isoforms is expected given that the location of the L6/60 binding site on amino acids 690–891 of mSlo1 is in an area encoded by an invariant exon encoding a polypeptide segment present in all 16 known mouse and rat Slo1 isoforms.

To address whether the microheterogeneity of Slo1 in rat brain is developmentally regulated, we performed immunoblots on crude membrane prepared from whole brains of different aged rats. This developmental immunoblot analysis revealed further heterogeneity in Slo1 polypeptides, with immunoreactive bands at M_r ≈ 135, 131 and 124 kD (bands 1, 2, 3 respectively in Fig. 2B). The components of the brain Slo1 pool change progressively with development, in that in the first two postnatal weeks the M_r ≈ 131 and 124 kD isoforms predominate, while in adult the M_r ≈ 135 kD isoform predominates. This suggests that the brain Slo1 polypeptide pool changes with development. However, precise correlation with specific splice variants (e.g. Strex exons) is not possible on the basis of electrophoretic mobility and immunoreactivity.

Immunolocalization of Slo1 in axons and terminal fields in the hippocampus

We next used the L6/60 mAb to evaluate localization of the Slo1 α subunit in rat brain. It has been reported previously that rat Slo1 is localized predominantly in axons and terminal fields of many brain regions, but is also present in certain neuronal somata and dendrites (Knaus et al., 1996; Hu et al., 2001; Grunnet and Kaufmann, 2004). Consistent with these studies, we found intense staining for Slo1 in the hilus of the dentate gyrus and in the stratum lucidum of CA3, corresponding to the mossy fiber axons of dentate granule cells (Fig. 3A). Moreover, Slo1 staining was observed in the middle and outer third of the molecular layer of the dentate gyrus, indicating Slo1 might be present on nerve terminals of perforant path axons. In stratum radiatum and stratum oriens of CA1–CA3 there is a less intensely staining zone of immunoreactivity that corresponds precisely to the termination zone of the Schaffer collateral pathway. There was virtually no labeling on the somata of dentate granule cells and pyramidal neurons in CA1 and CA3 regions (Fig. 3A).

To further verify specificity of L6/60 antibody, mouse brain sections from wild-type and Slo1-deficient mice were stained with mAb L6/60. L6/60 strongly labeled the hippocampus in sections obtained from the brains of wild-type mice, but not those from Slo1-deficient mice. Fig. 3B shows double immunofluorescence staining for Slo1 (red) and the voltage-gated K^+ channel Kv2.1 (green) in the anterior hippocampal formation in wild-type and Slo1 knockout mice. Kv2.1 is expressed on the somatodendritic membrane of interneurons and pyramidal neurons throughout this regions the hippocampus (Rhodes et al., 2004). In wild-type mice, Slo1 staining is restricted to the mossy fiber axons and terminal fields where it forms a staining pattern complementary to that of somatodendritic Kv2.1. In Slo1-deficient mice, Slo1 staining is eliminated but Kv2.1 staining is unchanged (Fig. 3B). Staining for the Kv1.4 channel (Sheng et al., 1992) was also unchanged in the Slo1-deficient mice (not shown). Combined with the fact that no obvious structural abnormalities are apparent by Nissl staining (A.M., unpublished data) the effects of the Slo1 knockout, at least at the level of these light microscope analyses, appear to be restricted to expression of Slo1 itself. It should be noted that the commercial anti-Slo1 antibodies used for the immunoblotting experiments in Fig. 1 did not yield immunohistochemical staining consistent with that of L6/60, or observed in previous studies of Slo1 localization. Moreover, the staining from the commercial anti-Slo1 antibodies was largely unaffected in the Slo1 knockout (data not shown).

Axonal localization of Slo1 was further confirmed by double-labeling immunofluorescence analysis using confocal microscopy. In the CA3 region of hippocampus, L6/60 labeling in stratum lucidum overlapped with staining for Kv1.4 (Fig. 4), which has been shown previously to be localized to mossy fiber axons and terminals in studies employing immunoelectron microscopy (Cooper et al., 1998) and experimental lesions of dentate gyrus and CA3 (Monaghan et al., 2001). In contrast, the Slo1 staining interdigitated with staining for Kv2.1 on the somata and apical dendrites of CA3 pyramidal neurons (Fig. 4).

To experimentally determine whether the L6/60 staining in stratum lucidum of CA3 was to mossy fiber axons and terminals, we employed the excitotoxin ibotenic acid to generate circumscribed lesions in the dentate gyrus of an individual hippocampus of adult rats. The hippocampus of the nonlesioned hemisphere served as the control. Sections from lesioned and control hemispheres were then stained with L6/60 and other antibodies to determine the effects of the dentate gyrus lesion. As shown in Fig. 5, L6/60 exhibits robust staining to an intense band in stratum lucidum of CA3 in a pattern consistent with localization to mossy fiber terminals and axons. Staining for Kv1.4 yields a similar pattern. That the staining for Slo1 is associated with axons and nerve terminals is supported by the fact that this staining is absent in sections prepared from the hemisphere in which the dentate gyrus had been lesioned. A similar loss of Kv1.4 staining was observed in the lesioned hemisphere,

consistent with previous results (Monaghan et al., 2001). Intense Slo1 staining is also observed in globus pallidus, presumably in termination zones of striatal efferents, as has also been previously observed for Kv1.4 (Sheng et al., 1992;Rhodes et al., 1997). The staining for Slo1 and for Kv1.4 in globus pallidus (and in other brain regions) was unaffected by the dentate gyrus lesion. These data showing specific loss of staining in the stratum lucidum of CA3 upon excitotoxic lesion of the dentate gyrus are consistent with a localization of Slo1 on axons and terminals of mossy fiber afferents that emanate from dentate granule cells that are selectively eliminated in the lesioned hemisphere.

Immunolocalization of Slo1 to basket cell axons and terminals in cerebellum

In the cerebellum, we found robust staining of Slo1 in the Purkinje cell and molecular layers (Fig. 6). Previous studies reported strong Slo1 staining in the somata and dendrites of Purkinje cells (Knaus et al., 1996;Sausbier et al., 2004). However, higher resolution imaging of this immunostaining with the L6/60 mAb revealed that in addition to robust somatodendritic staining of Purkinje cells, there was also intense labeling in the pinceau of basket cell terminals that surround the axon initial segments of Purkinje cells (Fig. 6). That the previously reported somatodendritic staining in Purkinje cells is less intense than staining on the basket cell terminals is shown by both immunofluorescence staining, and also by comparing results obtained using different development times in immunoperoxidase staining experiments (supplemental Fig. 1). Fig. 6B shows that the Slo1 staining in basket cell terminals, in Purkinje cells somata, and in the molecular layer is eliminated in the cerebella of Slo1 knockout mice, consistent with the specific nature of the staining.

To further investigate the localization of Slo1 in cerebellar cortex, double label immunofluorescence staining was combined with confocal microscopy. L6/60 consistently labeled the basket cell nerve terminals synapsing on Purkinje cells (Fig. 7A), where it exhibited strong overlap with intense staining for the Kv1.2 channel (McNamara et al., 1993;Rhodes et al., 1997). However, L6/60 staining did not precisely overlap, and in fact encircled staining for neurofascin 155/186 (NF-155) (Fig. 7B) that labeled the axon initial segments of Purkinje cells (Boiko et al., 2001;Ango et al., 2004). These high resolution confocal images also provide further support for expression of Slo1 on the somata and dendrites of Purkinje cells, as shown by double staining with calbindin (Fig. 7C), a Ca^{2+}-binding proteins expressed at high levels in Purkinje cells (Ango et al., 2004), and for somatodendritic Kv2.1 (Fig. 7D).

Axonal and presynaptic localization of endogenous Slo1, and exogenous recombinant human Slo1, in cultured rat hippocampal pyramidal neurons

To investigate whether exogenously expressed recombinant Slo1 α subunits would display a polarized localization in neurons, as observed in polarized epithelial cells (Bravo-Zehnder et al., 2000), we transfected primary cultures of rat hippocampal neurons (Lim et al., 2001). This culture system provides relatively homogenous population of pyramidal neurons (≈90%), which spontaneously form synaptic connections. These cultured rat hippocampal pyramidal neurons express endogenous Slo1, as judged by immunofluorescence staining of the soma, and of MAP-2 negative processes, presumably axons, with the L6/60 antibody (Fig. 8A). Map-2 positive processes, presumably dendrites, also exhibit detectable L6/60 staining.

To determine the localization of exogenous Slo1 in these cultured neurons, neurons were transfected with a human Slo1 (hSlo) cDNA (Accession number AAB65837, human isoform 5) containing an extracellular N-terminal Myc tag (Meera et al., 1997), at 8 days *in vitro* (DIV) and cultured until 11 DIV. We initially stained permeabilized neurons with L6/60 antibody (Fig. 8B) and anti-Myc antibody (data not shown) and found that majority of

hSlo1 was localized in the somata and proximal dendrites of transfected neurons, presumably in the rough endoplasmic reticulum as this perinuclear staining overlapped with the staining for BiP, a resident protein of this organelle (data not shown). However, surface labeling of hSlo1 in non-permeabilized neurons with anti-Myc antibody (see supplemental Fig. 2) revealed surface expression of hSlo1 and showed that the major surface pool of hSlo1 resides on the axonal membrane, where staining overlaps with that of the axonal marker, tau (Fig. 8C), and does not overlap with the dendritic marker Map-2 (Fig. 8D). Note the staining of myc-positive axons enveloping a presumably untransfected neuron (arrow) to the upper left of the transfected neuron in Fig. 8B, reinforcing the notion that the even the punctate staining on the somata and dendrites of cultured neurons may be due to Slo1 localization on afferent axons and terminals.

We further analyzed the localization of this surface pool of hSlo1 in cultured neurons. To examine whether surface hSlo1 localizes at the synaptic terminals as in the hippocampus *in situ*, neurons were double labeled with anti-Myc and anti-synapsin I antibodies under non-permeabilized and permeabilized conditions, respectively. At 11 DIV (i.e. 3 days after transfection), neurons expressing hSlo1 showed cell surface Myc-positive axonal processes projecting to neighboring cells. Although the surface Myc staining appeared as a punctate pattern on these processes, most of the puncta at 11 DIV did not overlap with synapsin-I positive puncta (Fig. 9A). By 14 DIV, a substantial subset of these cell-surface Myc-positive puncta were now found colocalized with the synapsin-I positive puncta (Fig. 9A and B). However, even at 14 DIV, a subpopulation of Myc-positive puncta did not colocalize with synapsin-I staining, indicating certain clusters of hSlo1 on the axonal membrane may represent immature nerve terminals without synapsin-I staining, similar to those that predominate at 11 DIV. While none of the surface Myc-positive puncta overlapped with postsynaptic staining of PSD-95 (Fig. 9B), some were opposed to PSD-95 puncta (arrows in Fig. 9B). These results suggest that axonal Slo1 channels become accumulated in presynaptic terminals as synapses mature in cultured neurons.

DISCUSSION

A determination of the precise localization of ion channel proteins is crucial to understanding their specific contribution to neuronal function, especially in the context of the extreme morphological complexity of mammalian central neurons (Trimmer and Rhodes, 2004). The distribution of Slo1 α subunits in mammalian brain has been studied previously by analyses of mRNA expression using *in situ* hybridization (Knaus et al., 1996; Chang et al., 1997) and immunostaining using polyclonal antibodies (Table I) raised against synthetic peptides (Knaus et al., 1996; Hu et al., 2001; Grunnet and Kaufmann, 2004; Martin et al., 2004) or fusion proteins (Sausbier et al., 2004) corresponding to segments from the Slo1 α subunit intracellular C-terminus. These studies revealed that Slo1 α subunits are expressed widely in rat brain but highly accumulated in axons and nerve terminals of principal neurons, a pattern that is most clearly observed in the hippocampus (Knaus et al., 1996). We have now generated an anti-Slo1 mAb, L6/60, that has been extensively characterized against recombinant Slo1 α subunits expressed in mammalian cell lines, and against brain samples from rats, and from wild-type and Slo1-deficient mice. Utilizing the L6/60 mAb in conjunction with mAbs for Kv channels and other neuronal proteins that show defined patterns of distribution in the hippocampus and cerebellum (Rhodes et al., 1997), and excitotoxic lesion studies (Monaghan et al., 2001), we further confirm the axonal and synaptic localization of Slo1 α subunit. Consistent with these previous studies, our results showed that Slo1 α subunits are expressed throughout the hippocampus and are localized to areas corresponding to axons and synaptic terminal zones, and are especially prominent in mossy fiber axons and terminals. The specificity of this staining is shown by

the fact that it is eliminated in Slo1-deficient mice, and in rats that have been subjected to experimental lesion of dentate granule cells, the source of mossy fibers.

Moreover, we provide compelling data that in cerebellum Slo1 exhibits prominent expression in the presynaptic terminals of cerebellar basket cells. This is in addition to lower levels of somatodendritic Slo1 expression in Purkinje cells as shown in previous immunocytochemical studies (Knaus et al., 1996; Grunnet and Kaufmann, 2004; Sausbier et al., 2004), and as suggested by electrophysiological studies of somatodendritic BK channels (e.g. Edgerton and Reinhart, 2003; Womack and Khodakhah, 2004). The high level of expression in basket cell terminals was substantiated using confocal immunofluorescence microscopy combined with double labeling with specific antibodies for marker proteins of different subcellular compartments (Rhodes et al., 1997; Ango et al., 2004). *In situ* hybridization experiments have shown that in cerebellum Slo1 mRNA is predominantly expressed in the Purkinje cell layer (Knaus et al., 1996; Chang et al., 1997). However, expression of Slo1 mRNA in basket cells, which lie close to the Purkinje cell layer, may be difficult to determine (Ango et al., 2004), such that Slo1 mRNA expression in basket cell somata could be masked by that in large cell bodies of Purkinje neurons in the *in situ* hybridization analyses. Slo1 KO mice are ataxic (Meredith et al., 2004; Sausbier et al., 2004), a phenotype that Sausbier et al. (2004) attributed to the lack of BK channels in Purkinje cells. However, the role of BK channels in the presynaptic terminals of basket cells may need to be considered to fully understand cerebellar dysfunction in Slo1 knockout mice. Sausbier et al (2004) found severe suppression of intrinsic Purkinje cell activity in Slo1-knockout mice. As basket cell terminals provide inhibitory drive to Purkinje cells, deletion of BK channels from these sites, and the resultant hyperexcitability of the GABAergic basket cell terminals, could further contribute to the suppressed intrinsic excitability of Purkinje cells and the ataxia observed in the Slo1-null mice. Such a model is consistent with results from Kv1.1 knockout mice, where loss of Kv1.1 from basket cell terminals increases GABA release to an extent sufficient to generate an ataxic phenotype due to suppression of Purkinje cell excitability (Zhang et al., 1999).

We show here that the validated anti-Slo1 L6/60 mAb recognizes multiple species of Slo1 in crude rat brain membrane preparations. Slo1 is subjected to alternative splicing to generate at least 11 isoforms in rats (NCBI accession number Q62976) and five isoforms in mouse (NCBI accession number Q08460). Moreover, some of these isoforms exhibit distinct patterns of phosphorylation, biophysical and trafficking properties, and expression (reviewed in Shipston, 2001). The binding site for L6/60 is in a region (a. a. 690–891 of mouse isoform 2) that is intact in all rat and mouse Slo1 isoforms, thus it is not surprising that this monospecific Slo1 mAb exhibits reactivity to multiple Slo1 species. That some of the heterogeneity of the L6/60-positive Slo1 pool is generated from alternative splicing is suggested by the fact that the observed microheterogeneity remains after exhaustive *in vitro* dephosphorylation of Slo1 with alkaline phosphatase. Our immunoblot analysis of samples prepared from the brains of different aged rats suggests that the alternative splicing may be developmentally regulated in brain. Anti-Slo1 mAbs that bind to discrete sites within isoform-specific polypeptide segments encoded by alternatively spliced Slo1 exons may allow for dissection of the brain Slo1 polypeptide pool.

We have presented here the first study using experimental excitotoxic lesions and knockout animals to definitively address the localization of Slo1 protein in mammalian brain. We have previously employed excitotoxic lesions in rat hippocampus to define the predominant subcellular localization of Kv1 channel α subunits to axons and presynaptic terminals (Monaghan et al., 2001), and of Kv2.1 and Kv4 α subunits to dendrites (Rhodes et al., 2004). Using antibodies to these channels as markers, we found here that ibotenic acid lesions in dentate gyrus eliminated anti-Slo1 L6/60 mAb staining in stratum lucidum of

CA3, consistent with a localization of Slo1 on axons and terminals of dentate granule cell mossy fibers, and not on dendrites of CA3 pyramidal neurons. These results are consistent with previous interpretation of light microscopic analyses of immunoperoxidase staining (Knaus et al., 1995; Grunnet and Kaufmann, 2004). Moreover, the presynaptic localization of Slo1 in mossy fiber terminals is similar to that defined in immunogold electron microscopic localization of Slo1 immunoreactivity to presynaptic terminals of another hippocampal circuit, the CA3-derived Schaffer collaterals that terminate in stratum radiatum of hippocampal CA1 (Hu et al., 2001). There is little doubt that Slo1/BK channels are found in somatodendritic membranes of most neurons, including cerebellar Purkinje cells neurons (e.g. Edgerton and Reinhart, 2003; Womack and Khodakhah, 2004), neocortical pyramidal neurons (Benhassine and Berger, 2005) and hippocampal CA1 pyramidal cells (Golding et al., 1999). The lack of detectable L6/60 staining in somatodendritic domains of adult hippocampal pyramidal neurons may reflect a substantially lower density of Slo1 protein here relative to that on axons and terminals, the presence of an as yet unknown splice variant that lacks L6/60 binding, or occlusion of L6/60 binding by protein-protein interactions or other post-translational modifications specific to the somatodendritic compartment.

We have expressed recombinant hSlo1 in cultured rat hippocampal neurons and showed that the exogenous hSlo1 α subunit was abundantly expressed on the axonal surface membrane, and that these surface hSlo1 channels became accumulated in presynaptic terminals as neuronal circuits mature *in vitro*. Although we can easily detect surface hSlo1 molecules expressed in these cultured hippocampal neurons, a large fraction of the translated hSlo1 was retained in the ER, as observed for endogenous Slo1 in these cultures, and as previously observed for wild-type hSlo1 expression in other non-neuronal heterologous systems (Bravo-Zehnder et al., 2000; Ling et al., 2003; Kwon and Guggino, 2004). We also observed somatodendritic staining of endogenous Slo1, and exogenous surface hSlo1 in these transfected neurons, suggesting that polarized expression of exogenous hSlo1 in neurons is not as tightly regulated as in epithelial cells (Bravo-Zehnder et al., 2000) or that overexpression of this protein normally found predominantly on axons and presynaptic terminals may overwhelm the axonal trafficking system, as has been observed for axonal Kv channels (Arnold and Clapham, 1999) and metabotropic glutamate receptors (Stowell and Craig, 1999) expressed exogenously in cultured neurons. That the level of surface hSlo1 staining in axons was clearly stronger than that in the somatodendritic region indicates that the prominent polarized localization of Slo1 in axons as observed in hippocampus was still established and maintained to a certain extent for exogenous hSlo1 in cultured neurons.

The Slo1 α subunit has a large cytoplasmic C-terminus that has been shown to be important for surface expression of Slo1 α subunit in heterologous expression system such as polarized Madin-Darby canine kidney (MDCK) cells (Bravo-Zehnder et al., 2000). This cytoplasmic tail also contains a signal for apical localization of a unique rabbit renal Slo1 isoform (NCBI accession number AF201702) in polarized mouse kidney cells (Kwon and Guggino, 2004). In most cases the apical membrane of polarized epithelial cells is analogous to the axonal membrane of neurons (and the basolateral to the somatodendritic; Dotti and Simons, 1990), although there are several axonal proteins which do not 'behave' (Trimmer, 1999; Trimmer and Rhodes, 2004). As the identified minimal sequence of the apical localization signal of the rabbit renal Slo1 (NAGQSRA) does not exhibit similarity to known trafficking and sorting signals (Kwon and Guggino, 2004), the molecular mechanisms of the polarized localization remains to be examined, especially in neuronal cells. It is intriguing that the NAGQSRA apical localization signal is found in all mouse and rat Slo1 isoforms.

Supplementary Material

Refer to Web version on PubMed Central for supplementary material.

Acknowledgments

LITERATURE CITED

Ango F, di Cristo G, Higashiyama H, Bennett V, Wu P, Huang ZJ. Ankyrin-based subcellular gradient of neurofascin, an immunoglobulin family protein, directs GABAergic innervation at purkinje axon initial segment. Cell. 2004; 119:257–272. [PubMed: 15479642]

Antonucci DE, Lim ST, Vassanelli S, Trimmer JS. Dynamic localization and clustering of dendritic Kv2.1 voltage-dependent potassium channels in developing hippocampal neurons. Neuroscience. 2001; 108:69–81. [PubMed: 11738132]

Arnold DB, Clapham DE. Molecular determinants for subcellular localization of PSD-95 with an interacting K+ channel. Neuron. 1999; 23:149–157. [PubMed: 10402201]

Banker GA, Cowan WM. Rat hippocampal neurons in dispersed cell culture. Brain Research. 1977; 126:397–425. [PubMed: 861729]

Bekele-Arcuri Z, Matos MF, Manganas L, Strassle BW, Monaghan MM, Rhodes KJ, Trimmer JS. Generation and characterization of subtype-specific monoclonal antibodies to K+ channel alpha- and beta-subunit polypeptides. Neuropharmacology. 1996; 35:851–865. [PubMed: 8938716]

Benhassine N, Berger T. Homogeneous distribution of large-conductance calcium-dependent potassium channels on soma and apical dendrite of rat neocortical layer 5 pyramidal neurons. Eur J Neurosci. 2005; 21:914–926. [PubMed: 15787698]

Benson DL, Watkins FH, Steward O, Banker G. Characterization of GABAergic neurons in hippocampal cell cultures. J Neurocytol. 1994; 23:279–295. [PubMed: 8089704]

Binder LI, Frankfurter A, Rebhun LI. The distribution of tau in the mammalian central nervous system. J Cell Biol. 1985; 101:1371–1378. [PubMed: 3930508]

Binder LI, Frankfurter A, Rebhun LI. Differential localization of MAP-2 and tau in mammalian neurons in situ. Ann N Y Acad Sci. 1986; 466:145–166. [PubMed: 3089105]

Boiko T, Rasband MN, Levinson SR, Caldwell JH, Mandel G, Trimmer JS, Matthews G. Compact myelin dictates the differential targeting of two sodium channel isoforms in the same axon. Neuron. 2001; 30:91–104. [PubMed: 11343647]

Boiko T, Van Wart A, Caldwell JH, Levinson SR, Trimmer JS, Matthews G. Functional specialization of the axon initial segment by isoform-specific sodium channel targeting. J Neurosci. 2003; 23:2306–2313. [PubMed: 12657689]

Bravo-Zehnder M, Orio P, Norambuena A, Wallner M, Meera P, Toro L, Latorre R, Gonzalez A. Apical sorting of a voltage- and Ca2+-activated K+ channel alpha -subunit in Madin-Darby canine kidney cells is independent of N-glycosylation. Proc Natl Acad Sci U S A. 2000; 97:13114–13119. [PubMed: 11069304]

Butler A, Tsunoda S, McCobb DP, Wei A, Salkoff L. mSlo, a complex mouse gene encoding "maxi" calcium-activated potassium channels. Science. 1993; 261:221–224. [PubMed: 7687074]

Chang CP, Dworetzky SI, Wang J, Goldstein ME. Differential expression of the alpha and beta subunits of the large-conductance calcium-activated potassium channel: implication for channel diversity. Brain Res Mol Brain Res. 1997; 45:33–40. [PubMed: 9105668]

Chen L, Tian L, MacDonald SH, McClafferty H, Hammond MS, Huibant JM, Ruth P, Knaus HG, Shipston MJ. Functionally diverse complement of large conductance calcium-and voltage-activated potassium channel (BK) alpha-subunits generated from a single site of splicing. J Biol Chem. 2005; 280:33599–33609. [PubMed: 16081418]

Collinson JM, Marshall D, Gillespie CS, Brophy PJ. Transient expression of neurofascin by oligodendrocytes at the onset of myelinogenesis: implications for mechanisms of axon-glial interaction. Glia. 1998; 23:11–23. [PubMed: 9562181]

Cooper EC, Milroy A, Jan YN, Jan LY, Lowenstein DH. Presynaptic localization of Kv1.4-containing A-type potassium channels near excitatory synapses in the hippocampus. J Neurosci. 1998; 18:965–974. [PubMed: 9437018]

Davis JQ, Lambert S, Bennett V. Molecular composition of the node of Ranvier: identification of ankyrin-binding cell adhesion molecules neurofascin (mucin+/third FNIII domain–) and NrCAM at nodal axon segments. J Cell Biol. 1996; 135:1355–1367. [PubMed: 8947556]

De Camilli P, Cameron R, Greengard P. Synapsin I (protein I), a nerve terminal-specific phosphoprotein. I. Its general distribution in synapses of the central and peripheral nervous system demonstrated by immunofluorescence in frozen and plastic sections. J Cell Biol. 1983; 96:1337–1354. [PubMed: 6404910]

Dotti CG, Simons K. Polarized sorting of viral glycoproteins to the axon and dendrites of hippocampal neurons in culture. Cell. 1990; 62:63–72. [PubMed: 2163770]

Drewe JA, Verma S, Frech G, Joho RH. Distinct spatial and temporal expression patterns of K+ channel mRNAs from different subfamilies. J Neurosci. 1992; 12:538–548. [PubMed: 1740690]

Du J, Tao-Cheng JH, Zerfas P, McBain CJ. K+ channel, Kv2.1, is apposed to astrocytic processes and is associated with inhibitory postsynaptic membranes in hippocampal and cortical principal neurons and inhibitory interneurons. Neuroscience. 1998; 84:37–848. [PubMed: 9522360]

Edgerton JR, Reinhart PH. Distinct contributions of small and large conductance Ca2+-activated K+ channels to rat Purkinje neuron function. J Physiol. 2003; 548:53–69. [PubMed: 12576503]

Evan GI, Lewis GK, Ramsay G, Bishop JM. Isolation of monoclonal antibodies specific for human c-myc proto-oncogene product. Mol Cell Biol. 1985; 5:3610–3616. [PubMed: 3915782]

Fury M, Marx SO, Marks AR. Molecular BKology: the study of splicing and dicing. Sci STKE 2002. 2002:PE12.

Golding NL, Jung HY, Mickus T, Spruston N. Dendritic calcium spike initiation and repolarization are controlled by distinct potassium channel subtypes in CA1 pyramidal neurons. J Neurosci. 1999; 19:8789–8798. [PubMed: 10516298]

Grunnet M, Kaufmann WA. Coassembly of big conductance Ca2+-activated K+ channels and L-type voltage-gated Ca2+ channels in rat brain. J Biol Chem. 2004; 279:36445–36453. [PubMed: 15210719]

Hu H, Shao LR, Chavoshy S, Gu N, Trieb M, Behrens R, Laake P, Pongs O, Knaus HG, Ottersen OP, Storm JF. Presynaptic Ca2+-activated K+ channels in glutamatergic hippocampal terminals and their role in spike repolarization and regulation of transmitter release. J Neurosci. 2001; 21:9585–9597. [PubMed: 11739569]

Hwang PM, Fotuhi M, Bredt DS, Cunningham AM, Snyder SH. Contrasting immunohistochemical localizations in rat brain of two novel K+ channels of the Shab subfamily. J Neurosci. 1993; 13:1569–1576. [PubMed: 8463836]

Kim E, Niethammer M, Rothschild A, Jan YN, Sheng M. Clustering of Shaker-type K+ channels by interaction with a family of membrane-associated guanylate kinases. Nature. 1995; 378:85–88. [PubMed: 7477295]

Knaus HG, Eberhart A, Koch RO, Munujos P, Schmalhofer WA, Warmke JW, Kaczorowski GJ, Garcia ML. Characterization of tissue-expressed alpha subunits of the high conductance Ca(2+)-activated K+ channel. J Biol Chem. 1995; 270:22434–22439. [PubMed: 7673230]

Knaus HG, Schwarzer C, Koch RO, Eberhart A, Kaczorowski GJ, Glossmann H, Wunder F, Pongs O, Garcia ML, Sperk G. Distribution of high-conductance Ca(2+)-activated K+ channels in rat brain: targeting to axons and nerve terminals. J Neurosci. 1996; 16:955–963. [PubMed: 8558264]

Kwon SH, Guggino WB. Multiple sequences in the C terminus of MaxiK channels are involved in expression, movement to the cell surface, and apical localization. Proc Natl Acad Sci U S A. 2004; 101:15237–15242. [PubMed: 15469924]

Lim ST, Antonucci DE, Scannevin RH, Trimmer JS. A novel targeting signal for proximal clustering of the Kv2.1 K+ channel in hippocampal neurons. Neuron. 2000; 25:385–397. [PubMed: 10719893]

Maletic-Savatic M, Lenn NJ, Trimmer JS. Differential spatiotemporal expression of K+ channel polypeptides in rat hippocampal neurons developing in situ and in vitro. J Neurosci. 1995; 15:3840–3851. [PubMed: 7751950]

McNamara NM, Muniz ZM, Wilkin GP, Dolly JO. Prominent location of a K+ channel containing the alpha subunit Kv 1.2 in the basket cell nerve terminals of rat cerebellum. Neuroscience. 1993; 57:1039–1045. [PubMed: 7508581]

Meera P, Wallner M, Song M, Toro L. Large conductance voltage- and calcium-dependent K+ channel, a distinct member of voltage-dependent ion channels with seven N-terminal transmembrane segments (S0–S6), an extracellular N terminus, and an intracellular (S9–S10) C terminus. Proc Natl Acad Sci U S A. 1997; 94:14066–14071. [PubMed: 9391153]

Martin G, Puig S, Pietrzykowski A, Zadek P, Emery P, Treistman S. Somatic localization of a specific large-conductance calcium-activated potassium channel subtype controls compartmentalized ethanol sensitivity in the nucleus accumbens. J Neurosci. 2004; 24:6563–6572. [PubMed: 15269268]

Meredith AL, Thorneloe KS, Werner ME, Nelson MT, Aldrich RW. Overactive bladder and incontinence in the absence of the BK large conductance Ca2+-activated K+ channel. J Biol Chem. 2004; 279:36746–36752. [PubMed: 15184377]

Misonou H, Mohapatra DP, Park EW, Leung V, Zhen D, Misonou K, Anderson AE, Trimmer JS. Regulation of ion channel localization and phosphorylation by neuronal activity. Nat Neurosci. 2004; 7:711–718. [PubMed: 15195093]

Misonou H, Trimmer JS. A primary culture system for biochemical analyses of neuronal proteins. J Neurosci Methods. 2005; 144:165–173. [PubMed: 15910974]

Monaghan MM, Trimmer JS, Rhodes KJ. Experimental localization of Kv1 family voltage-gated K+ channel alpha and beta subunits in rat hippocampal formation. J Neurosci. 2001; 21:5973–5983. [PubMed: 11487620]

Murakoshi H, Shi G, Scannevin RH, Trimmer JS. Phosphorylation of the Kv2.1 K+ channel alters voltage-dependent activation. Mol Pharmacol. 1997; 52:821–828. [PubMed: 9351973]

Orio P, Rojas P, Ferreira G, Latorre R. New disguises for an old channel: MaxiK channel beta-subunits. News Physiol Sci. 2002; 17:156–161. [PubMed: 12136044]

Petersen JD, Chen X, Vinade L, Dosemeci A, Lisman JE, Reese TS. Distribution of postsynaptic density (PSD)-95 and Ca2+/calmodulin-dependent protein kinase II at the PSD. J Neurosci. 2003; 23:11270–11278. [PubMed: 14657186]

Pyott SJ, Glowatzki E, Trimmer JS, Aldrich RW. Extrasynaptic localization of inactivating calcium-activated potassium channels in mouse inner hair cells. J Neurosci. 2004; 24:9469–9474. [PubMed: 15509733]

Rasband MN, Park EW, Zhen D, Arbuckle MI, Poliak S, Peles E, Grant SG, Trimmer JS. Clustering of neuronal potassium channels is independent of their interaction with PSD-95. J Cell Biol. 2002; 159:663–672. [PubMed: 12438413]

Rhodes KJ, Carroll KI, Sung MA, Doliveira LC, Monaghan MM, Burke SL, Strassle BW, Buchwalder L, Menegola M, Cao J, An WF, Trimmer JS. KChIPs and Kv4 alpha subunits as integral components of A-type potassium channels in mammalian brain. J Neurosci. 2004; 24:7903–7915. [PubMed: 15356203]

Rhodes KJ, Strassle BW, Monaghan MM, Bekele-Arcuri Z, Matos MF, Trimmer JS. Association and colocalization of the Kvbeta1 and Kvbeta2 beta-subunits with Kv1 alpha-subunits in mammalian brain K+ channel complexes. J Neurosci. 1997; 17:8246–8258. [PubMed: 9334400]

Sah P, Faber ES. Channels underlying neuronal calcium-activated potassium currents. Prog Neurobiol. 2002; 66:345–353. [PubMed: 12015199]

Sausbier M, Hu H, Arntz C, Feil S, Kamm S, Adelsberger H, Sausbier U, Sailer CA, Feil R, Hofmann F, Korth M, Shipston MJ, Knaus HG, Wolfer DP, Pedroarena CM, Storm JF, Ruth P. Cerebellar ataxia and Purkinje cell dysfunction caused by Ca2+-activated K+ channel deficiency. Proc Natl Acad Sci U S A. 2004; 101:9474–9478. [PubMed: 15194823]

Schafer DP, Bansal R, Hedstrom KL, Pfeiffer SE, Rasband MN. Does paranode formation and maintenance require partitioning of neurofascin 155 into lipid rafts? J Neurosci. 2004; 24:3176–3185. [PubMed: 15056697]

Sheng M, Tsaur ML, Jan YN, Jan LY. Subcellular segregation of two A-type K+ channel proteins in rat central neurons. Neuron. 1992; 9:271–284. [PubMed: 1497894]

Sheng M, Liao YJ, Jan YN, Jan LY. Presynaptic A-current based on heteromultimeric K+ channels detected in vivo. Nature. 365:72–75. [PubMed: 8361540]

Shi G, Kleinklaus AK, Marrion NV, Trimmer JS. Properties of Kv2.1 K+ channels expressed in transfected mammalian cells. J Biol Chem. 1994; 269:23204–23211. [PubMed: 8083226]

Shi G, Trimmer JS. Differential asparagine-linked glycosylation of voltage-gated K+ channels in mammalian brain and in transfected cells. J Membr Biol. 1999; 168:265–273. [PubMed: 10191360]

Shipston MJ. Alternative splicing of potassium channels: a dynamic switch of cellular excitability. Trends in Cell Biology. 2001; 11:353–359. [PubMed: 11514177]

Stowell JN, Craig AM. Axon/dendrite targeting of metabotropic glutamate receptors by their cytoplasmic carboxy-terminal domains. Neuron. 1999; 22:525–536. [PubMed: 10197532]

Strassle BW, Menegola M, Rhodes KJ, Trimmer JS. Light and electron microscopic analysis of KChIP and Kv4 localization in rat cerebellar granule cells. J Comp Neurol. 2005

Szendrei GI, Lee VM, Otvos L Jr. Recognition of the minimal epitope of monoclonal antibody Tau-1 depends upon the presence of a phosphate group but not its location. J Neurosci Res. 1993; 34:243–249. [PubMed: 7680727]

Tian L, Duncan RR, Hammond MS, Coghill LS, Wen H, Rusinova R, Clark AG, Levitan IB, Shipston MJ. Alternative splicing switches potassium channel sensitivity to protein phosphorylation. J Biol Chem. 2001; 276:7717–7720. [PubMed: 11244090]

Tiffany AM, Manganas LN, Kim E, Hsueh Y-P, Sheng M, Trimmer JS. PSD-95 and SAP-97 exhibit distinct mechanisms for regulating K+ channel surface expression and clustering. J Cell Biol. 2000; 148:147–157. [PubMed: 10629225]

Trimmer JS. Immunological identification and characterization of a delayed rectifier K+ channel polypeptide in rat brain. Proc Natl Acad Sci U S A. 1991; 88:10764–10768. [PubMed: 1961744]

Trimmer JS. Sorting out receptor trafficking. Neuron. 1999; 22:411–412. [PubMed: 10197517]

Trimmer JS, Rhodes KJ. Localization of voltage-gated ion channels in mammalian brain. Annu Rev Physiol. 2004; 66:477–519. [PubMed: 14977411]

Tsaur ML, Sheng M, Lowenstein DH, Jan YN, Jan LY. Differential expression of K+ channel mRNAs in the rat brain and down-regulation in the hippocampus following seizures. Neuron. 1992; 8:1055–1067. [PubMed: 1610565]

Veh RW, Lichtinghagen R, Sewing S, Wunder F, Grumbach IM, Pongs O. Immunohistochemical localization of five members of the Kv1 channel subunits: contrasting subcellular locations and neuron-specific co-localizations in rat brain. Eur J Neurosci. 1995; 7:2189–2205. [PubMed: 8563969]

Wang H, Kunkel DD, Martin TM, Schwartzkroin PA, Tempel BL. Heteromultimeric K+ channels in terminal and juxtaparanodal regions of neurons. Nature. 1993; 365:75–79. [PubMed: 8361541]

Wang H, Kunkel DD, Schwartzkroin PA, Tempel BL. Localization of Kv1.1 and Kv1.2, two K channel proteins, to synaptic terminals, somata, and dendrites in the mouse brain. J Neurosci. 1994; 14:4588–4599. [PubMed: 8046438]

Weiger TM, Hermann A, Levitan IB. Modulation of calcium-activated potassium channels. J Comp Physiol A Neuroethol Sens Neural Behav Physiol. 2002; 188:79–87. [PubMed: 11919690]

Zhang CL, Messing A, Chiu SY. Specific alteration of spontaneous GABAergic inhibition in cerebellar purkinje cells in mice lacking the potassium channel Kv1. 1. J. Neurosci. 1999; 19:2852–2864. [PubMed: 10191303]

Zhou XB, Arntz C, Kamm S, Motejlek K, Sausbier U, Wang GX, Ruth P, Korth M. A molecular switch for specific stimulation of the BKCa channel by cGMP and cAMP kinase. J Biol Chem. 2001; 276:43239–43245. [PubMed: 11514553]
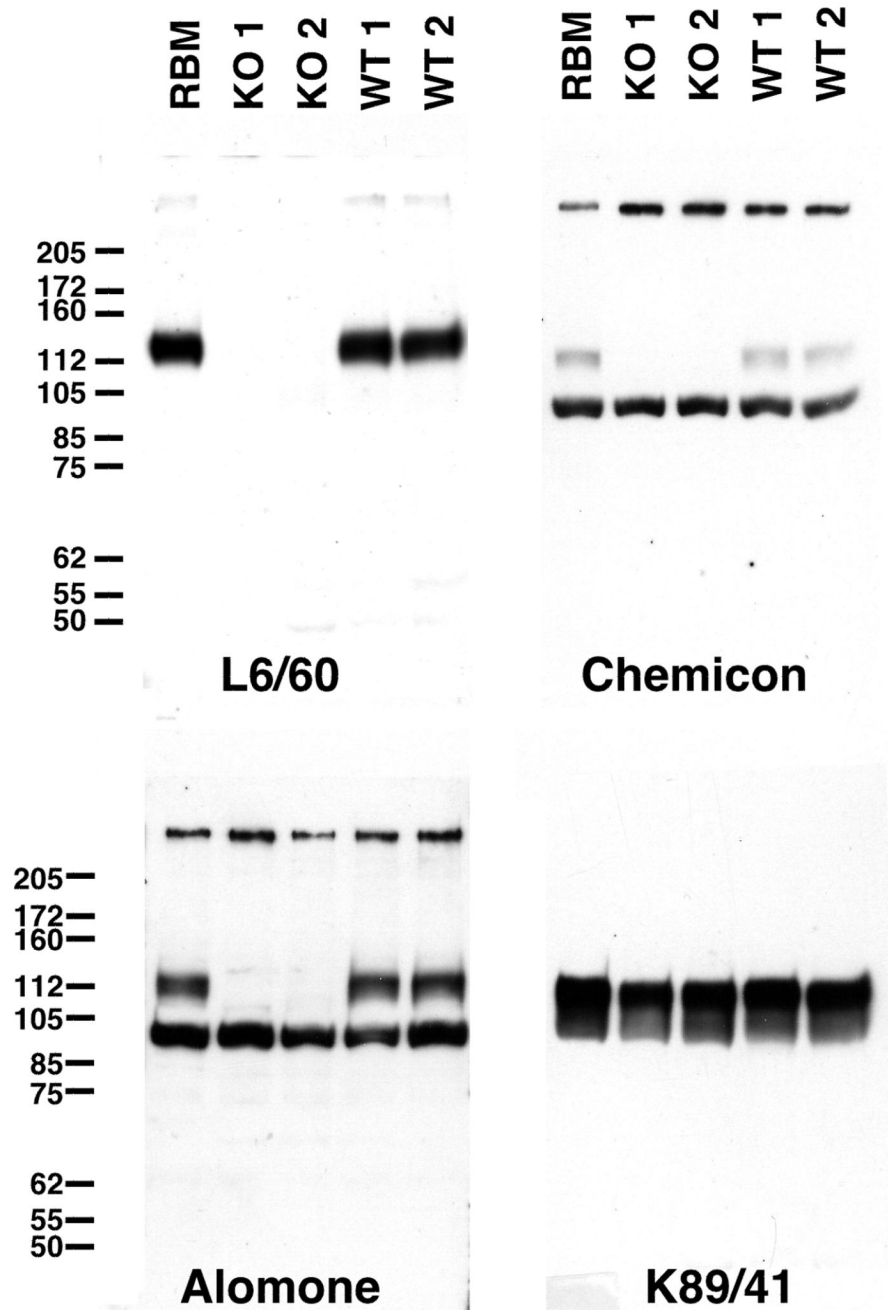
**Fig. 1. Specificity of the anti-Slo1 mAb L6/60**
A, immunoblot analysis of brain membrane fractions from adult rats, and wild-type and Slo1-deficient mice. Proteins were fractionated on 7.5% SDS-PAGE and transferred to nitrocellulose membranes and probed with mouse monoclonal (L6/60, 10 µg/ml) or rabbit polyclonal anti-Slo1 (Alomone, 1:500; Chemicon, 1:200), or mouse monoclonal anti-Kv2.1 (K89/41, TC supe 1:2) antibodies as noted. Numbers to left denote mobility of prestained molecular weight standards in kD.
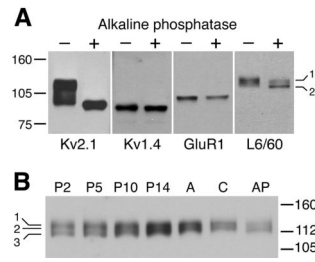
Fig. 2. Microheterogeneity of Slo1 in rat brain revealed by L6/60 immunoblot analyses
A: Immunoblot analysis of the effects of alkaline phosphatase (AP) digestion on adult rat brain Slo1. Adult rat brain membranes treated without (−) or with 0.1 U/ml AP (+) for 3 h at 37°C were separated on 7.5% SDS-PAGE and transferred to nitrocellulose membranes, then probed with anti-Kv2.1 (K89/41 mouse mAb, TC supe 1:2), anti-Kv1.4 (K13/31 mouse mAb, TC supe 1:2), anti-GluR1 (rabbit polyclonal antibody, Upstate 1:1000), or anti-Slo1 (L6/60, 10 µg/ml) antibodies. Slo1 exhibited AP- shifts from $M_r \approx 135$ to ≈ 128 kD (bands 1 and 2 indicated on the right). Brain Kv2.1 also shifted in M_r upon AP treatment, whereas Kv1.4 and GluR1 did not. **B:** Immunoblot analysis of developmental rat brain membrane samples. L6/60 (10 µg/ml) immunostaining at postnatal day 2 (P2) revealed at least three distinct bands as indicated in the left margin (1, 135 kD; 2, 131 kD; 3, 124 kD), which changed in their relative proportions during postnatal development. A=adult, C=adult sample incubated 3 h at 37°C without AP, AP=adult sample incubated 3 h at 37°C with AP. Numbers to left denote mobility of prestained molecular weight standards in kD.
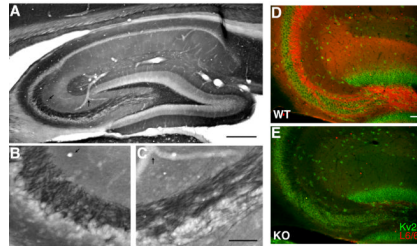
Fig. 3. Immunolocalization of Slo1 in hippocampus
A–C: L6/60 staining in adult rat hippocampus **A:** overview of L6/60 (0.6 µg/ml) immunoperoxidase staining in hippocampus. **B, C:** higher magnification images of the staining shown in A. **B:** stratum lucidum of the CA3 region of the hippocampus. **C:** magnified view of mossy fiber axons. Arrows in **A–C** highlight anatomical landmarks that specify the regions magnified. **D–E:** double label immunofluorescence labeling of brain sections from wild-type (**D**, WT) and Slo1-deficient (**E**, KO) mice. Brain sections from these mice were stained with L6/60 (24 µg/ml) mAb in red, and anti-Kv2.1 (KC rabbit polyclonal, 1:100) antibody in green. Images were taken from the hilus of the dentate gyrus and CA3 stratum lucidum. Scale bars, **A:**, 500 µm; **B, C:** 100 µm; **D:** 50 µm.
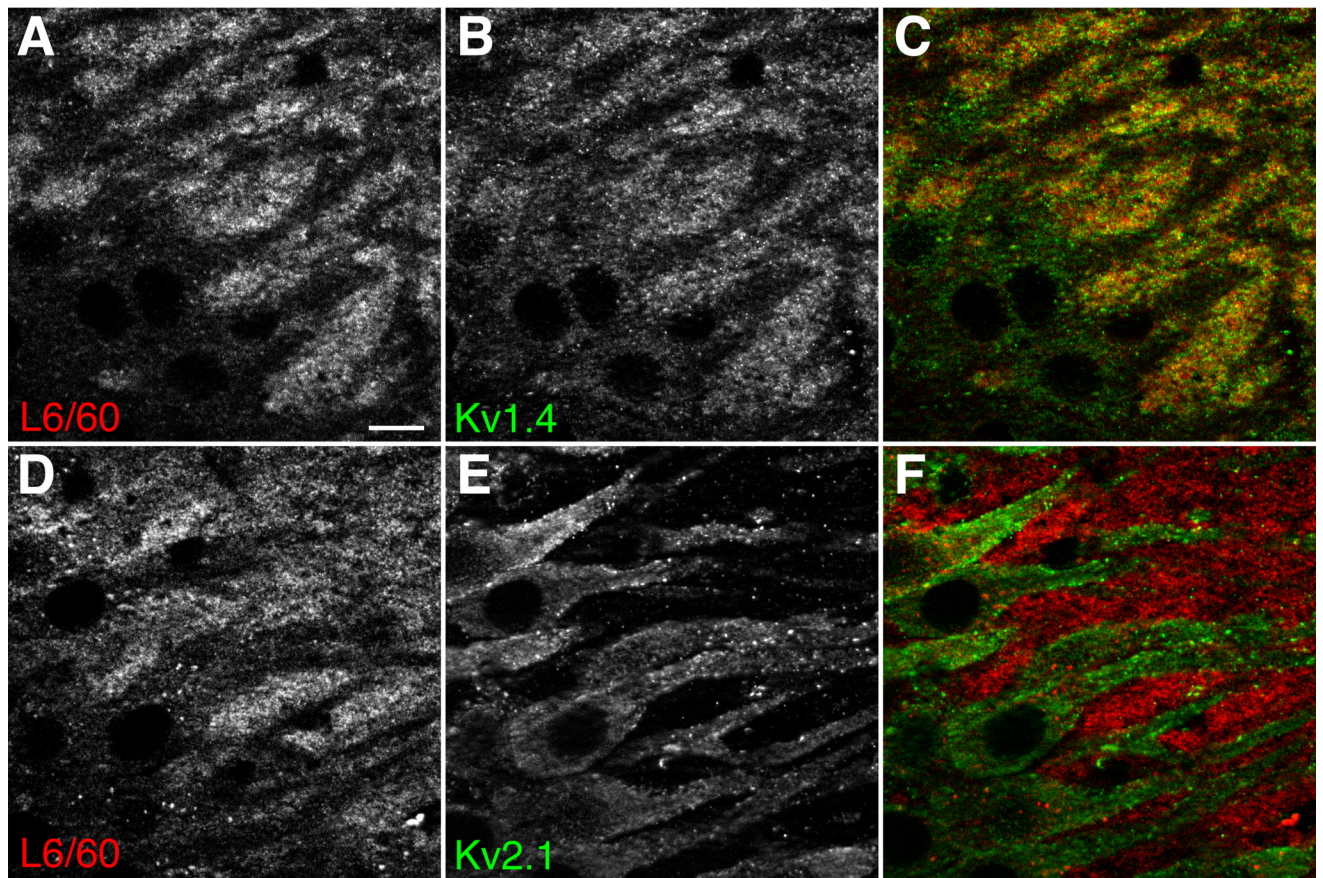
**Fig. 4. Localization of Slo1 in hippocampal mossy fibers**
Magnified view of stratum lucidum of CA3 region of hippocampus. **A–C**: somata and apical dendrites of CA3 pyramidal neurons were negatively stained with L6/60 (**A**, 24 µg/ml) as well as with anti-Kv1.4 antibody (**B**, K13/31 mouse mAb, TC supe 1:2), which overlapped in mossy fibers (**C**). **D–F**: in contrast, somatodendritic Kv2.1 (**D**, KC rabbit polyclonal antibody, 1:100) staining interdigitated with L6/60 staining (E), indicating the presence of Slo1 on synaptic terminals on the Kv2.1-positive apical dendrites of CA3 pyramidal neurons (F, overlay). Scale bars, 10 µm.
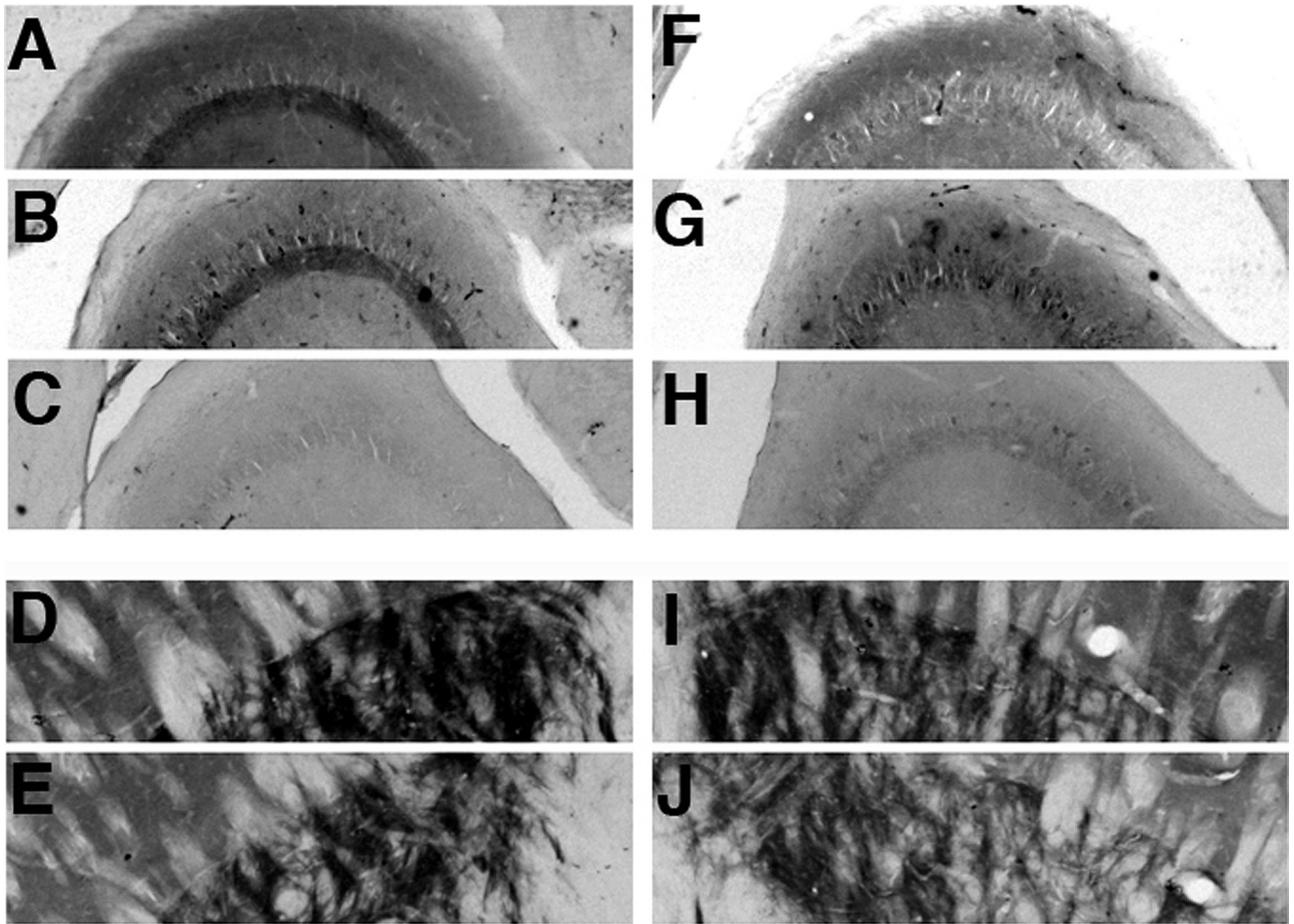
Fig. 5. Effects of an ibotenic acid lesion on the distribution and density of Slo1 immunoreactivity in the hippocampal formation

These photomicrographs show the pattern of immunoreactivity for the indicated subunits in the unoperated, control hemisphere (**A–E**) and operated hemisphere (**F–J**) of an animal that sustained a circumscribed unilateral ibotenic acid lesion. This lesion destroyed cells in the distal CA1 subfield, prosubiculum and subiculum, and also destroyed a central portion of the dentate gyrus. The entire CA3 and proximal CA1 subfield was spared by this lesion. This lesion greatly reduced the density of Slo1 (**A, F**; L6/60 TC supe 1:10), and Kv1.4 (**B, G**; K13/31 TC supe 1:10) in stratum lucidum of CA3, but did not affect binding of secondary antibody alone (**C, H**), nor staining for Slo1 (**D**, I; L6/60 TC supe 1:10), and Kv1.4 (**E, J**; K13/31 TC supe 1:10) in the terminal fields of striatal effernts to globus pallidus.
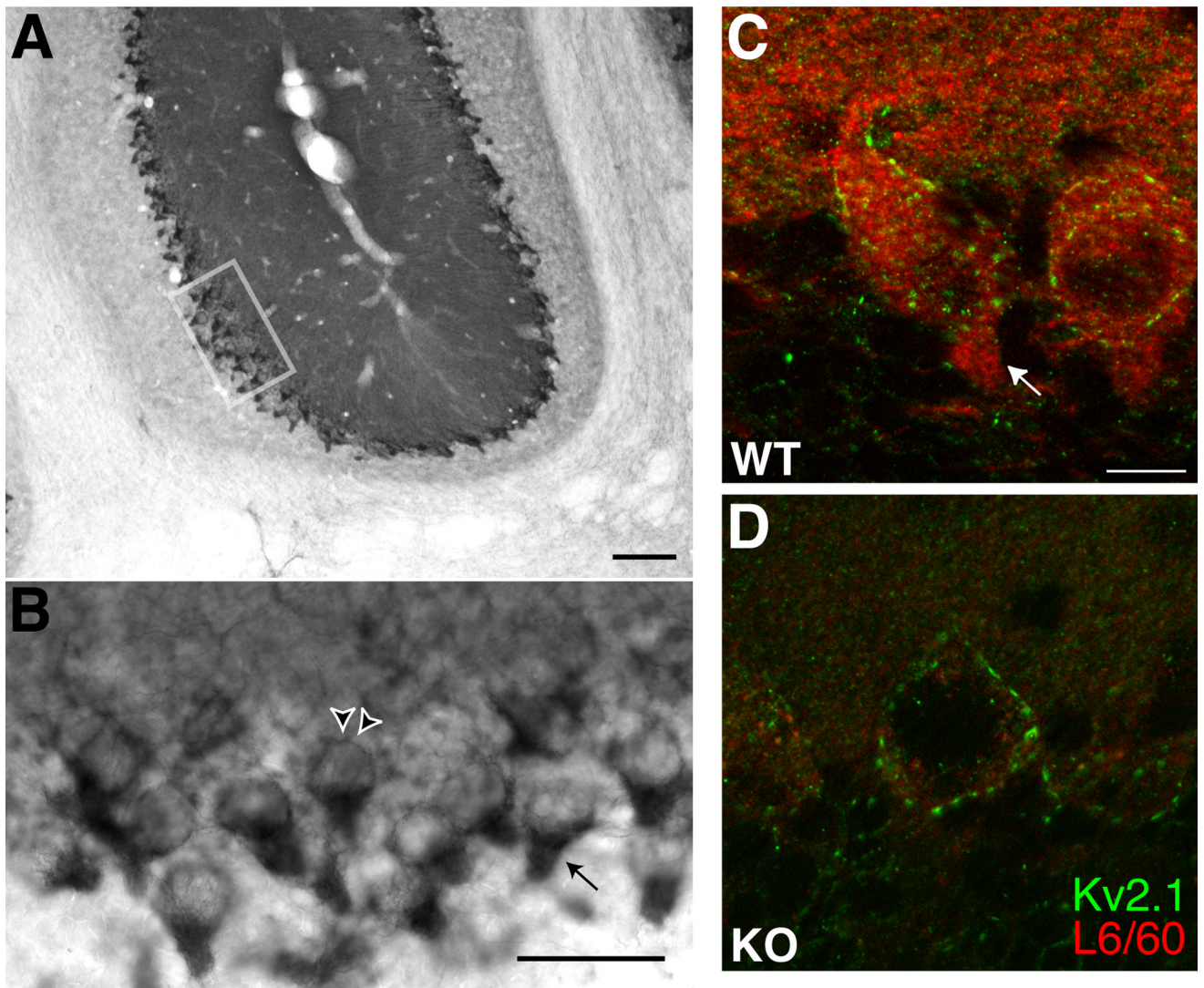
Fig. 6. Slo1 staining in cerebellum
A: low magnification view of L6/60 (0.6 µg/ml) immunoperoxidase staining near the primary fissure. Note moderate to high levels of staining in the molecular layer relative to the granule cell layer, and intense staining at/near the Purkinje cell layer. **B:** higher magnification view of the area boxed in A, showing intense L6/60 staining in the Purkinje cell layer. The arrowheads point to a Purkinje cell soma, while the arrow points to a basket cell pinceau terminal onto a Purkinje cell initial segment. **C–D:** Double label immunofluorescence staining of brain sections from wild-type (**C:** WT) and Slo1-deficient (**D:** KO) mice. Brain sections from these mice were stained with L6/60 mAb (24 µg/ml) in red, and anti-Kv2.1 (KC rabbit polyclonal, 1:100) antibody in green. Images were taken from the Purkinje cell layer and reveal that staining in Purkinje cell somata, basket cell terminals, and the molecular layer is eliminated in the Slo1 knockout. Scale bars, **A:,** 100 µm; **B, C:** 500 µm; **D:** 10 µm.
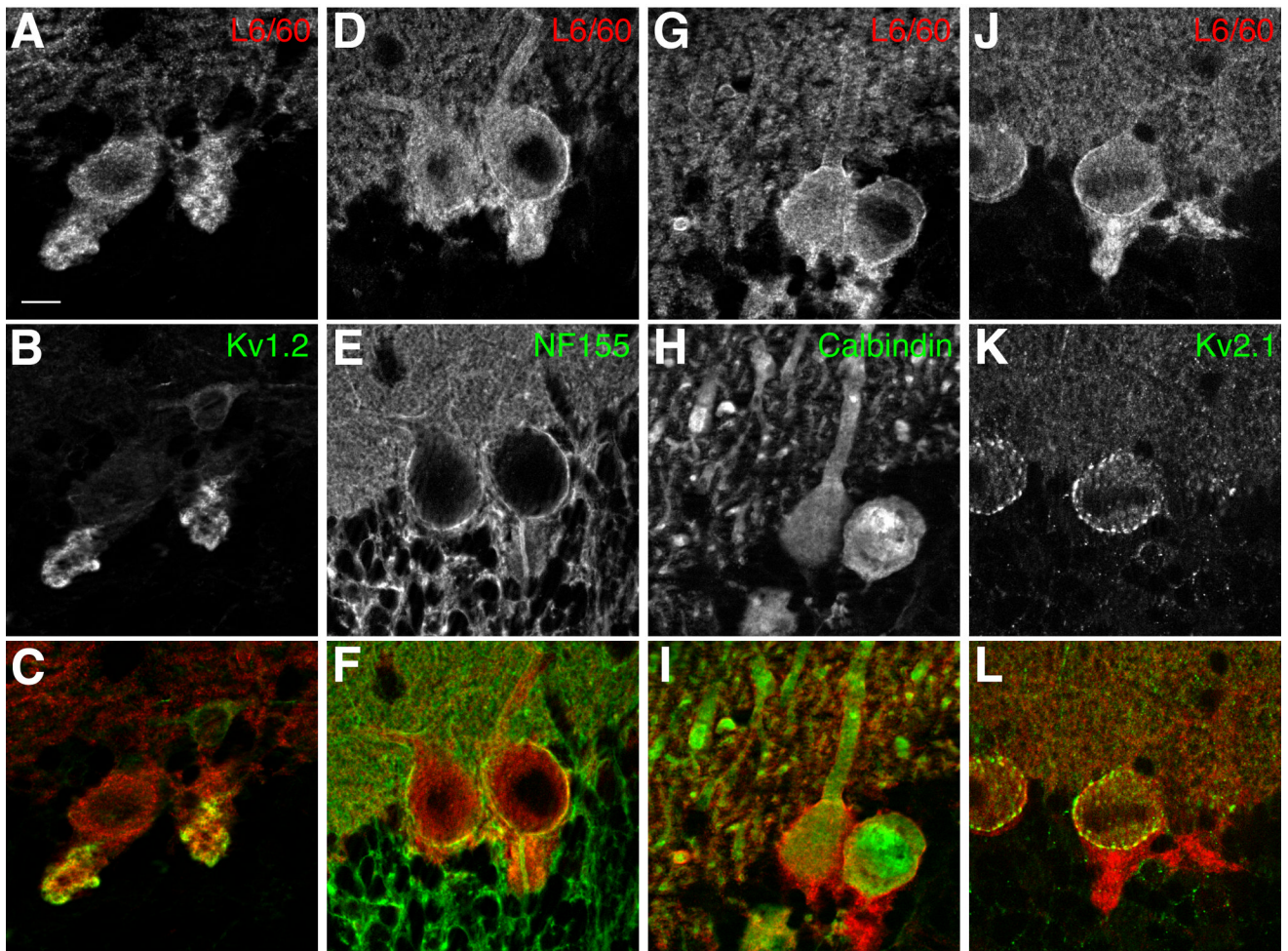
**Fig. 7. Slo1 localization in the cerebellar Purkinje cell layer**
Confocal images of double label immunofluorescence staining. **A–C:** Slo1 and Kv1.2 localization in basket cell terminals. L6/60 (**A:** 24 µg/ml) staining overlaps with that for Kv1.2 (**B:** K14/16 mouse mAb, 16 µg/ml) in basket cell terminals (**C:** overlay); **D–F:** L6/60 (**D:** 24 µg/ml) staining encircles axon initial segments of Purkinje cells, stained with anti-NF-155/186 antibody (**E:** L11A/41 mouse mAb, TC supe 1:2; **F:** overlay). **G–H:** dendrites of multiple Purkinje cells, filled with anti-calbindin (**H:** Sigma mouse monoclonal, 16 µg/ml) staining, were associated with membrane-associated L6/60 staining (**G:** 24 µg/ml; **I:** overlay). **J–L:** localization of Slo1 in Purkinje cell somata. Slo1 staining (**J:** L6/60; 24 µg/ml) on the somata of Purkinje cells partially overlapped with Kv2.1 (**K:** KC rabbit polyclonal antibody, 1:100) surface clusters (**L:** overlay). Scale bars, 10 µm.
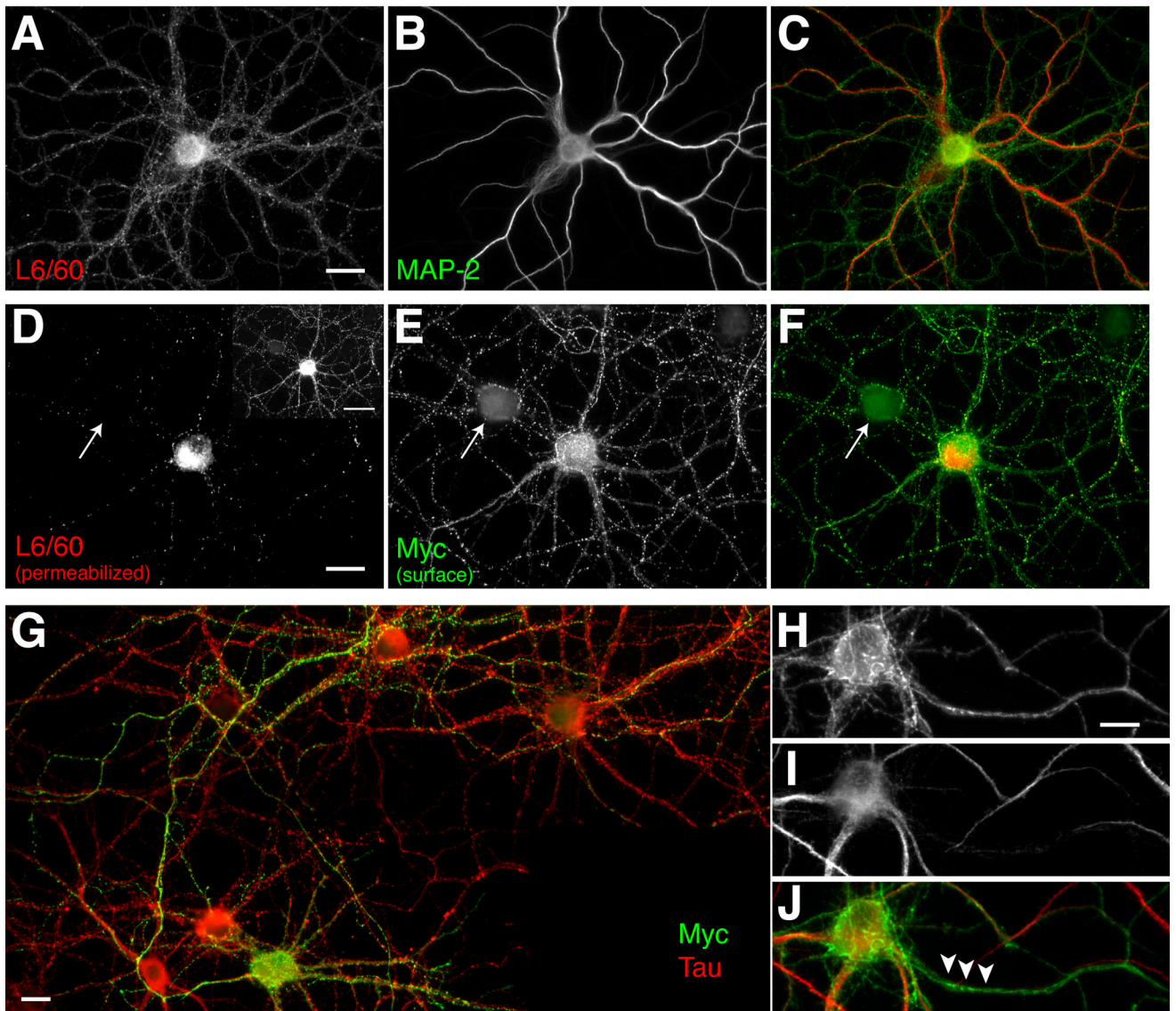
Fig. 8. Axonal localization of endogenous Slo1, and exogenous recombinant human Slo1, (hSlo1) in cultured rat hippocampal pyramidal neurons

A–C: Localization of endogenous Slo1. Neurons at 24 DIV were fixed, permeabilized with 0.1% Triton X-100 and stained with anti-Slo1 antibody L6/60 (**A:** 24 µg/ml; green) to detect the total pool of endogenous rSlo1, and anti-MAP2 (**B:** Sigma mouse mAb, 1:1000; **C:** overlay). **D–F:** Localization of surface hSlo1. Neurons at 11 DIV were fixed, stained with anti-Myc antibody (**E:** mouse monoclonal 1-9E10, 1 µg/ml) for cell surface hSlo1 (green), and then permeabilized with 0.1% Triton X-100 for L6/60 (**D:** 5 µg/ml) staining (red) to detect the total pool of exogenous hSlo1 and endogenous rSlo1 (**F:** overlay). Arrow points to a presumably untransfected neuron in the culture. Panel **D** inset: hSlo in both axons and dendrites was detected on a longer exposure. **G:** Surface Myc-positive (mouse mAb 19E10, 1 µg/ml) processes overlap with axonal tau (Sigma mouse monoclonal antibody 1:2000) staining. **H–J:** Surface Myc-positive (**H:** mouse mAb 19E10, 1 µg/ml) processes do not overlap with dendritic MAP-2 (**I:** Sigma mouse mAb, 1:1000) staining (**J:** overlay). Scale bars, **A–F:**, 20 µm; **D inset:** 50 µm ; **G:** 10 µm; **H–J:** 10 µm.
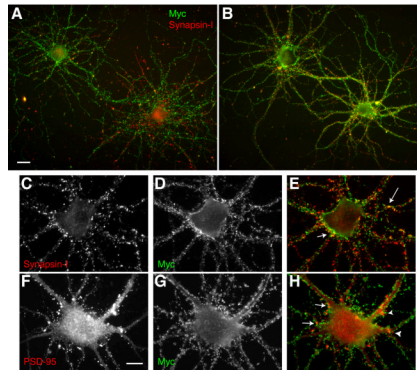
Fig. 9. Presynaptic localization of human Slo1 in cultured hippocampal pyramidal neurons
A–B: Developmental changes of surface hSlo1 staining. Neurons at 11 DIV (**A**) and 14 DIV (**B**) were fixed, stained with anti-Myc antibody (mouse mAb 19E10, 1 µg/ml; green), and then permeabilized with 0.1% Triton X-100 for presynaptic synapsin-I staining (Sigma rabbit polyclonal antibody, 1:1000; red). Yellow signal indicates overlap between surface Myc and synapsin-I staining. Scale bar, 20 µm. **C–H:** Presynaptic but not postsynaptic localization of surface hSlo1. Non-permeabilized neurons were stained with anti-Myc antibody (**D, G:** mouse mAb 19E10, 1 µg/ml; green), and then permeabilized with 0.1% Triton X-100 for presynaptic synapsin-I (**C:** Sigma rabbit polyclonal antibody, 1:1000; red) staining (**E:** overlay) or postsynaptic PSD-95 (**F:** K28/43 mouse mAb, TC supe 1:10) staining (**H:** overlay). Scale bars, **A–B:**, 20 µm; **C–H:** 10 µm.
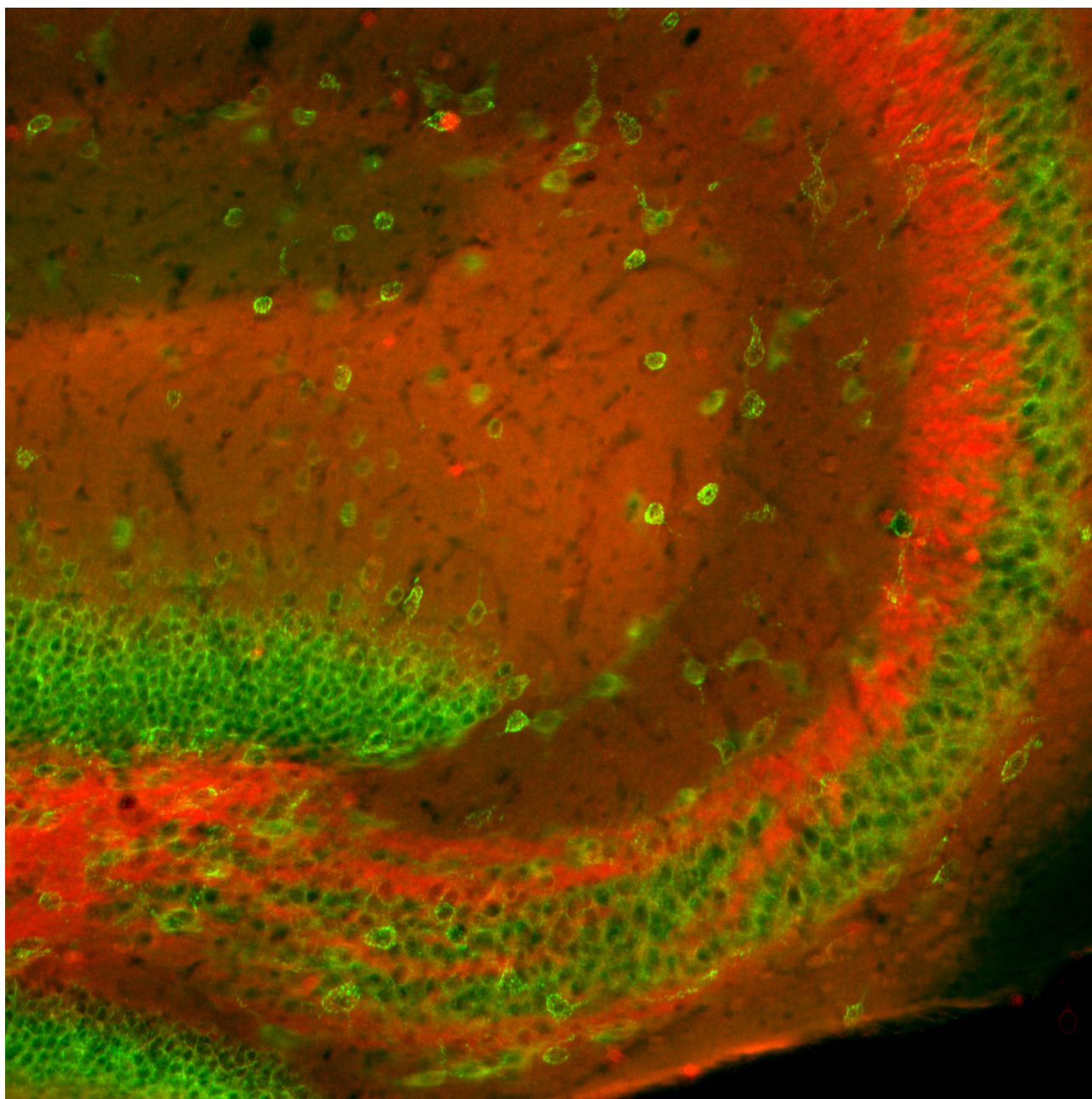
Fig. 10.

Table 1

Summary of Slo1 Antibodies

Anti-slo1 antibodies used in this study	
L6/60 mouse monoclonal IgG2a	GST Fusion protein 690–1196 Mapped to within 690–891
Alomone APC-021, lot AN-04 Rabbit polyclonal	GST Fusion protein 1098–1196
Chemicon AB5228, lot 22040170 Rabbit polyclonal	GST Fusion protein 1098–1196
Anti-slo1 antibodies used in other studies	
Martin et al., 2004. Affinity Bioreagents PA1-923 rabbit polyclonal	Synthetic peptide 913–926
Knaus et al., 1996; Hu et al., 2001, Grunnet & Kaufman, 2004 rabbit polyclonal	Synthetic peptide 913–926
Sausbier et al., 2004 rabbit polyclonal	GST Fusion protein 674–1115

Amino acid positions correspond to original mSlo sequence of Butler et al., 1993 (NCBI accession number AAA39746